WIF-B Cells: An In Vitro Model for Studies of Hepatocyte Polarity

Gudrun Ihrke,* Edward B. Neufeld,‡ Tim Meads,§ Michael R. Shanks,* Doris Cassio,‖ Michael Laurent,‖ Trina A. Schroer,§ Richard E. Pagano,‡ and Ann L. Hubbard*

*Department of Cell Biology and Anatomy, The Johns Hopkins School of Medicine, Baltimore, Maryland 21205; ‡Department of Embryology, Carnegie Institution of Washington, Baltimore, Maryland 21210; §Department of Biology, Johns Hopkins University, Baltimore, Maryland 21218; and ‖Centre National de la Recherche Scientifique, URA 1343, Institut Curie, Biologie, Université de Paris-Sud, 91405 Orsay, Cedex, France

Abstract. We have evaluated the utility of the hepatoma-derived hybrid cell line, WIF-B, for in vitro studies of polarized hepatocyte functions. The majority (>70%) of cells in confluent culture formed closed spaces with adjacent cells. These bile canalicular-like spaces (BC) accumulated fluorescein, a property of bile canaliculi in vivo. By indirect immunofluorescence, six plasma membrane (PM) proteins showed polarized distributions similar to rat hepatocytes in situ. Four apical PM proteins were concentrated in the BC membrane of WIF-B cells. Microtubules radiated from the BC (apical) membrane, and actin and foci of γ-tubulin were concentrated in this region. The tight junction-associated protein ZO-1 was present in belts marking the boundary between apical and basolateral PM domains. We explored the functional properties of this boundary in living cells using fluorescent membrane lipid analogs and soluble tracers. When cells were incubated at 4°C with a fluorescent analog of sphingomyelin, only the basolateral PM was labeled. In contrast, when both PM domains were labeled by de novo synthesis of fluorescent sphingomyelin from ceramide, fluorescent lipid could only be removed from the basolateral domain. These data demonstrate the presence of a barrier to the lateral diffusion of lipids between the PM domains. However, small soluble FITC-dextrans (4,400 mol wt) were able to diffuse into BC, while larger FITC-dextrans were restricted to various degrees depending on their size and incubation temperature. At 4°C, the surface labeling reagent sNHS-LC-biotin (557 mol wt) had access to the entire PM, but streptavidin (60,000 mol wt), which binds to biotinylated molecules, was restricted to only the basolateral domain. Such differential accessibility of well-characterized probes can be used to mark each membrane domain separately. These results show that WIF-B cells are a suitable model to study membrane trafficking and targeting in hepatocytes in vitro.

In vitro–polarized cell systems have been successfully exploited to study membrane traffic in epithelial cells. MDCK cells (McRoberts et al., 1981) are a prominent in vitro model for kidney epithelium, as Caco-2 cells (Pinto et al., 1983) are for enterocytes. In contrast, no polarized line derived from hepatocytes has been available. Hepatocytes represent an extreme in the spectrum of protein-sorting routes in epithelial cells, because they appear to lack a direct pathway to the apical surface. They deliver newly synthesized plasma membrane (PM)[1] proteins first to the basolateral membrane and then transport molecules destined for the apical domain across the cell via transcytosis (Bartles et al., 1987; Schell et al., 1992). A valid in vitro model would facilitate further characterization of sorting events in hepatocytes and allow comparisons among different epithelial cell types. Although the isolated perfused liver retains the in situ tissue architecture, its use in vitro is limited. Only short term experiments are possible, and the presence of other cell types confounds results when probes that are organelle but not cell type specific are used. Hepatoma lines are often differen-

Drs. Ihrke and Neufeld contributed equally to this study.

Address all correspondence to Ann L. Hubbard, Department of Cell Biology and Anatomy, Johns Hopkins School of Medicine, 725 North Wolfe Street, Baltimore, MD 21205.

1. *Abbreviations used in this paper*: APN, aminopeptidase N; BC, bile canalicular-like spaces; C_5-DMB-, N-[5(5,7-dimethyl BODIPY)-1-pentanoyl]-; C_5-DMB-Cer, N-[5-(5,7-dimethyl BODIPY)-1-pentanoyl]-D-*erythro*-sphingosine; C_5-DMB-SM, N-[5-(5,7-dimethyl BODIPY)-1-pentanoyl]-D-*erythro*-sphingosylphosphorylcholine; DF-BSA, defatted BSA; DPPIV, dipeptidyl peptidase IV; HBFM, Hepes-buffered biotin- and serum-free medium; HSFM, Hepes-buffered serum-free medium; LSCM, laser scanning confocal microscopy; 5'NT, 5'-nucleotidase; pAb, polyclonal antibody; PM, plasma membrane; sNHS-LC-Biotin, sulfosuccinimidyl-6-(biotin-amido) hexanoate.

tiated but not well polarized, as they exhibit few or no apical bile canalicular-like structures, the functional equivalent of the networks of branching channels into which bile is secreted in vivo (Porvaznik et al., 1976; Rogier et al., 1986; Maurice et al., 1988; Chiu et al., 1990). This problem has been partially overcome by fusing rat hepatoma cells (Fao) and human fibroblasts (WI38), thus generating hybrid cells that express liver-specific functions after specific chromosome segregation (Cassio et al., 1991). The WIF12-1 cells produced by this approach also exhibit substantial polarity. However, they only grow to a low maximal density and many cells remain unpolarized. Consequently, a derivative of these cells, designated WIF-B, was selected specifically for its ability to grow to a high density (Shanks, M., D. Cassio, O. Lecoq, and A. Hubbard, manuscript submitted for publication).

The present study was designed to evaluate the polarized phenotype of WIF-B cells. Specifically, we examined the steady state distribution of six domain-specific PM proteins, the architecture of the cytoskeleton, and the localization of the tight junction–associated protein ZO-1. Functional properties of the boundaries between apical and basolateral domains in living cells were examined by using fluorescent lipid analogs, soluble extracellular tracers, and a membrane impermeant labeling reagent. Our results show that the vast majority of WIF-B cells are highly polarized and exhibit functional tight junctions. Therefore, the WIF-B line appears to be a suitable model for in vitro studies of membrane traffic and transcytosis. (Portions of this work have been published in abstract form [Cassio, D., M. Shanks, G. Ihrke, M. Laurent, and A. L. Hubbard. 1992. *Mol. Biol. Cell.* 3:304a].)

Materials and Methods

Medium nutrient mixture F-12 (Ham's modified), formula No. 92-5054EA, was obtained from GIBCO-BRL (Gaithersburg, MD); FCS was supplied from Hyclone (Logan, UT); rhodamine-labeled phalloidin, *N*-[5-(5,7-dimethyl BODIPY)-1-pentanoyl]-D-*erythro*-sphingosine (C_5-DMB-Cer) and *N*-[5-(5,7-dimethyl BODIPY)-1-pentanoyl]-D-*erythro*-sphingosylphosphorylcholine (C_5-DMB-SM) was purchased from Molecular Probes, Inc. (Eugene, OR); SM-2-Bio-Beads were from Bio-Rad Laboratories (Rockville Center, NY); sulfosuccinimidyl-6-(biotinamido) hexanoate (sNHS-LC-Biotin) were from Pierce (Rockford, IL); streptavidin and FITC-streptavidin were obtained from Jackson ImmunoResearch Laboratories, Inc. (West Grove, PA); fluorescein diacetate, FITC-conjugated dextrans, and all other chemicals were from Sigma Immunochemicals (St. Louis, MO).

Cell Culture

WIF-B cells were cultured in a humidified 7% CO_2/93% air incubator at 37°C as described elsewhere (Shanks, M., D. Cassio, O. Lecoq, and A. Hubbard, manuscript submitted for publication). Briefly, cells were grown in modified Ham's F12 medium (Coon and Weiss, 1969) supplemented with HAT (10^{-5} M hypoxanthine, 4×10^{-8} M aminopterin, 1.6×10^{-6} M thymidine) and 5% FCS. Cells were routinely passaged on plastic dishes (Falcon Plastics, Cockneysville, PA) at 1.6–3.8 $\times$ 10^4/cm^2. For experiments cells were plated onto plastic dishes or glass coverslips at 3.8×10^4 cells/cm^2. We used 10–14-d-old cultures in all experiments, since the cells reached their maximal density and polarity at this time (Shanks et al., submitted for publication). That is, they occupied 80–95% of the dish surface area, and 80–95% of the cells participated in forming one or more phase-lucent, spherical structures when observed by phase contrast microscopy. By several criteria at least 90% of these spaces were located between cells (see Results); we have termed these intercellular structures bile canicular-like spaces (BC).

Indirect Immunofluorescence

PM Antigens and ZO-1. The mAbs against aminopeptidase N (APN), dipeptidyl peptidase IV (DPPIV), HA4, CE9, and HA321 have been described (Bartles et al., 1985*a*; Hubbard et al., 1985; Scott and Hubbard, 1992), as have been the rabbit polyclonal antibodies (pAbs) to these antigens (Bartles et al., 1985*a*; Bartles et al., 1985*b*; Scott and Hubbard, 1992; Hoppe and Hubbard, 1985). Guinea pigs pAbs to affinity-purified DPPIV and CE9 (Bartles et al., 1985*a*) were prepared commercially (HRP, Inc., Denver, PA). Mouse mAbs (5NE5, 5N4-2, and 5NH3) and the rabbit pAb to 5′-nucleotidase (5′NT) were a generous gift of Dr. Paul Luzio (University of Cambridge, Cambridge, U.K.) (Siddle et al., 1981; Bailyes et al., 1984), and the rat anti-ZO-1 mAb a gift of Dr. Bruce Stevenson (University of Alberta, Edmonton, Canada) (Stevenson et al., 1986). Fluorescent secondary antibodies were from Dako (Santa Barbara, CA), Kirkegaard & Perry (Gaithersburg, MD), Jackson ImmunoResearch Laboratories Inc. (West Grove, PA), Pasteur Production (Marne la Coquette, France), or Sigma Immunochemicals as indicated.

Cells grown on coverslips were fixed in 3% paraformaldehyde in PBS and permeabilized with methanol at 4°C as described elsewhere (Mevel-Ninio and Weiss, 1981). After rehydration in PBS, cells were incubated in primary antibody(s) (mAbs 1:100, pAbs 1:200–400 in PBS, 1% BSA), washed in PBS and then incubated with goat anti-mouse, goat anti-rabbit, or goat anti-guinea pig IgG coupled to FITC or Texas red (1:50–100), and mounted in PBS, 25% glycerol containing 2 mg/ml *p*-phenylenediamine. In double labeling experiments, the cells were incubated with both primary or both secondary antibodies at the same time. Confocal pictures were taken on a Bio-Rad MRC 600 confocal imaging system with a 63X objective (Carl Zeiss, Oberkochen, Germany) using Bio-Rad CoMOS or SOM software.

Cytoskeletal Proteins. The mouse mAb to α-tubulin (clone DM1A) was from Sigma Immunochemicals. The rabbit pAb to a *Xenopus* γ-tubulin fusion protein was a gift from Dr. Tim Stearns (Stanford University, Stanford, CA) (Stearns et al., 1991). Secondary antibodies from Vector Labs Inc. (Burlingame, CA) or Kirkegaard & Perry Laboratories, Inc. (Gaithersburg, MD) were used and gave similar results.

Microtubules and actin were localized in cells grown on cover slips fixed in 3.5% paraformaldehyde in PBS for 10 min at 37°C, briefly rinsed in PBS, and then extracted in −20°C acetone for 5 min. After rehydrating in PBS containing 15 mM glycine, cells were incubated with anti-α-tubulin (1:500 in PBS, 0.5% BSA), washed in PBS, and then incubated with horse anti-mouse FITC-IgG (1:100). The cells were washed again, incubated with 10 U/ml rhodamine-labeled phalloidin in PBS for 30 min, washed in PBS for 1 min, and then mounted in Mowiol containing 2.5% 1,4-diazobicyclo-(2,2,2)-octane. Microtubules and γ-tubulin were double labeled in cells fixed in −20°C methanol for 5 min. The anti-γ-tubulin pAb was diluted 1:100 and the anti-α-tubulin mAb used as above. Secondary antibodies were goat anti-rabbit FITC-IgG and goat anti-mouse TRITC-IgG, respectively; antibody incubations and washes were as before. Pictures were taken with a Zeiss Axiovert microscope equipped with a 100× objective (Zeiss).

Labeling of Living Cells

Fluorescein Diacetate. Cultures grown on plastic dishes were incubated with fluorescein diacetate at a final concentration of 0.1 μg/ml for 20 min at 37°C, and then washed two times with serum-free medium at 2°C (Rotman and Papermaster, 1966). The cells were observed and photographed within 10 min on a Zeiss Axioplan fluorescence microscope using a 25× water immersion lens under phase contrast or epifluorescence illumination. Fluorescent BC were counted on micrographs and expressed as percent of total number of BC seen by phase contrast.

Fluorescent Lipids

Preparation of Fluorescent Lipid/BSA Complexes. Complexes of fluorescent lipid with defatted BSA (DF-BSA) were prepared as described (Pagano and Martin, 1988), and subsequently diluted to 5 μM with Hepes-buffered, serum-free medium (HSFM), pH 7.2, without penicillin/streptomycin, amphotericin B, or HAT. Concentrations of lipid stock solutions were determined by reference to known concentrations of fluorescent standards.

Incubation of Cells with Fluorescent Lipid. Cultures grown on coverslips were washed with HSFM at 2°C, incubated with 5 μM C_5-DMB-SM/DF-BSA in HSFM for 30 min at 2°C, and washed at 2°C, before observation and photography. Cultures incubated with C_5-DMB-Cer/DF-BSA as above were washed and further incubated in HSFM at 37°C for 60 min. To remove fluorescent lipid associated with the PM, cells were incubated 6 × 10 min at 10°C with 5% DF-BSA ("back-exchange").

Quantification of Fluorescent Apical PM Domain Labeling. Cultures grown on glass coverslips and incubated with 5 μM C_5-DMB-SM/DF-BSA as described were maintained at 2°C before observation under the micro-

scope. BC were first identified under phase contrast illumination, and then categorized as fully, partially, or unlabeled (see Results and Fig. 6) under epifluorescence illumination using a Zeiss Laser Scanning Confocal Microscope equipped with a 100× objective and fluorescein optics. Seven different sets were examined (four cover glass preparations per set, 8–10 fields per cover glass). Each cover glass preparation was examined within 5–10 min after mounting on a glass microscope slide.

FITC-Dextrans

FITC-dextrans were diluted in serum-free medium to a final concentration of 10 mg/ml. 10 ml aliquots were dialyzed against 21 serum-free medium containing SM-2 Bio-Beads at 4°C in the dark with three medium changes and stored at 4°C until use. Cells grown on plastic dishes were washed once with serum-free medium, incubated with FITC-dextrans for either 10 min at 37°C or for 60 min at 2°C, and washed two times with serum-free medium at 2°C, before observation and microscopy (see "Fluorescein Diacetate").

Biotinylation

Cells grown to confluency on coverslips (10–12 d) were washed three times with cold PBS^+ (PBS, 0.9 mM $CaCl_2$, 0.52 mM $MgCl_2$, 0.16 $MgSO_4$, pH 7.2) and once with cold biotinylation buffer (10 mM borate, 137 mM NaCl, 3.8 mM KCl, 0.9 mM $CaCl_2$, 0.52 mM $MgCl_2$, and 0.16 mM $MgSO_4$, pH 9.0). Cells were labeled with sNHS-LC-biotin (0.62 mg/ml in biotinylation buffer) twice for 15 min at 4°C. The reaction was stopped with serum- and biotin-free medium buffered with 20 mM Hepes, pH 7.2 (HBFM). Cells were washed once again with HBFM and then incubated with or without 50 μg/100 μl streptavidin in HBFM for 30 min on ice. Cells were rinsed once with PBS^+, incubated for 5–10 min in HBFM, washed three times with PBS^+, and fixed as described for immunofluorescence of PM proteins. Cells were then incubated with FITC-conjugated streptavidin (20 μg/ml) for 30 min at room temperature, washed with PBS, and mounted in PBS, 50% glycerol containing 2 mg/ml *p*-phenylenediamine. Cells were examined on a Zeiss Laser Scanning Confocal Microscope equipped with a 100× objective lens. Fluorescence images were captured in the laser scanning mode and phase contrast images were photographed using the conventional mode of the microscope.

Results

WIF-B Cells Are Highly Polarized

Under optimal culture conditions, WIF-B cell monolayers exhibit many phase-lucent structures (Fig. 1), about two to three times more than the parent WIF12-1 cells (Shanks et al., manuscript submitted for publication). Although these spherical spaces look very different from the branching bile canaliculi that are a hallmark of the hepatocyte apical domain in vivo (Motta et al., 1978), they are functionally and compositionally analogous. We confirmed this in two ways: by showing that organic anions accumulate in these structures as they do in WIF12-1 cells (Cassio et al., 1991), and by localizing several well-characterized apical membrane proteins to their surrounding PM domains.

Transcellular Transport of Organic Anions. Fluorescein has commonly been used to demonstrate hepatic uptake and excretion of organic anions into the bile in vivo (Hanzon, 1952; Bhathal and Christie, 1969). Confluent WIF-B cultures were incubated with non-fluorescent fluorescein diacetate for 20 min at 37°C, washed, and examined immediately by fluorescence microscopy for appearance of fluorescein, the hydrolysis product of fluorescein diacetate. The vast majority (80–90%) of the phase-lucent spaces were fluorescent (Fig. 1). There was also some diffuse fluorescence within the cells, which was more prominent in the first minutes of incubation (data not shown). The bile acid derivative FITC-glycocholate, when added to the medium at 37°C, also accumulated in most of these structures (data not shown). These results demonstrate that WIF-B cells are capable of vectorial transport of at least two different classes of molecules secreted into bile in vivo. Moreover, it indicates that the presumed bile canalicular transporters reside in the membrane surrounding the phase-lucent spaces.

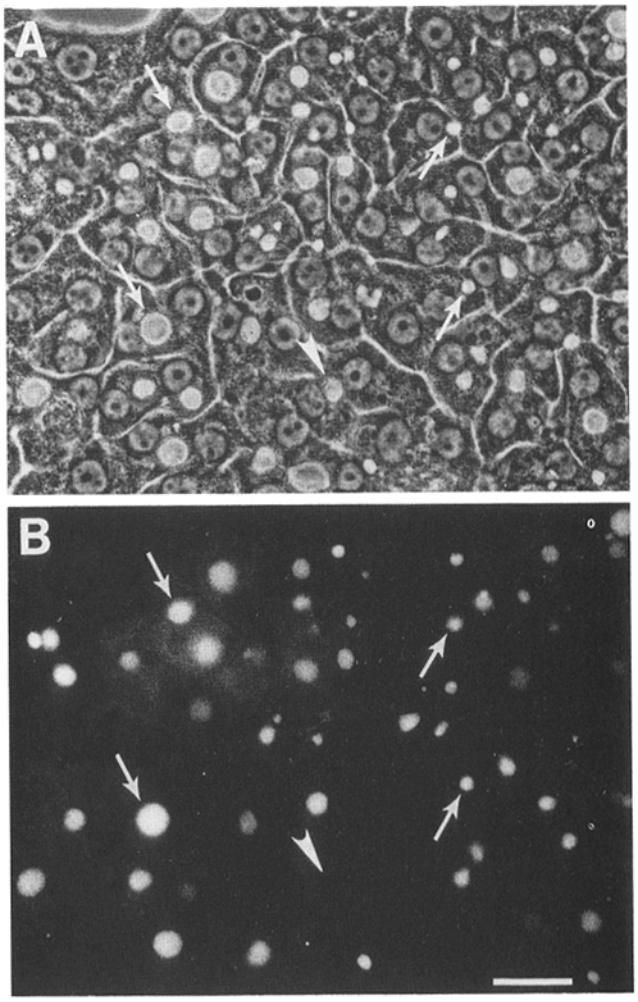

Figure 1. The organic anion fluorescein accumulates in WIF-B BC. 12-d-old confluent cultures were incubated with 0.1 μg/ml fluorescein diacetate in complete medium for 20 min at 37°C, washed, and then photographed within 10 min by phase contrast (*A*) or epifluorescence optics (*B*). 91% of the phase-lucent areas are fluorescent (*arrows*), indicating that fluorescein diacetate has been taken up and hydrolyzed to fluorescein, which is then excreted into the BC. The arrowhead points to an unlabeled BC. Bar, 25 μm.

Distribution of PM Proteins. We next studied the distribution of several PM proteins using immunofluorescence laser scanning confocal microscopy (LSCM). The apical PM protein APN was confined to the membranes of the phase-lucent structures, while the basolateral protein CE9 showed a complementary localization (Fig. 2). Three other apical PM proteins, DPPIV, HA4, and the glycosylphosphatidylinositol-linked 5′NT, also exhibited distributions similar to APN. All were concentrated in the limiting membrane of these phase-lucent structures, while another basolateral marker, HA321, was excluded. The structures that appeared as translucent "holes" with conventional phase contrast optics (Fig. 1) could clearly be seen as enclosed spaces by LSCM

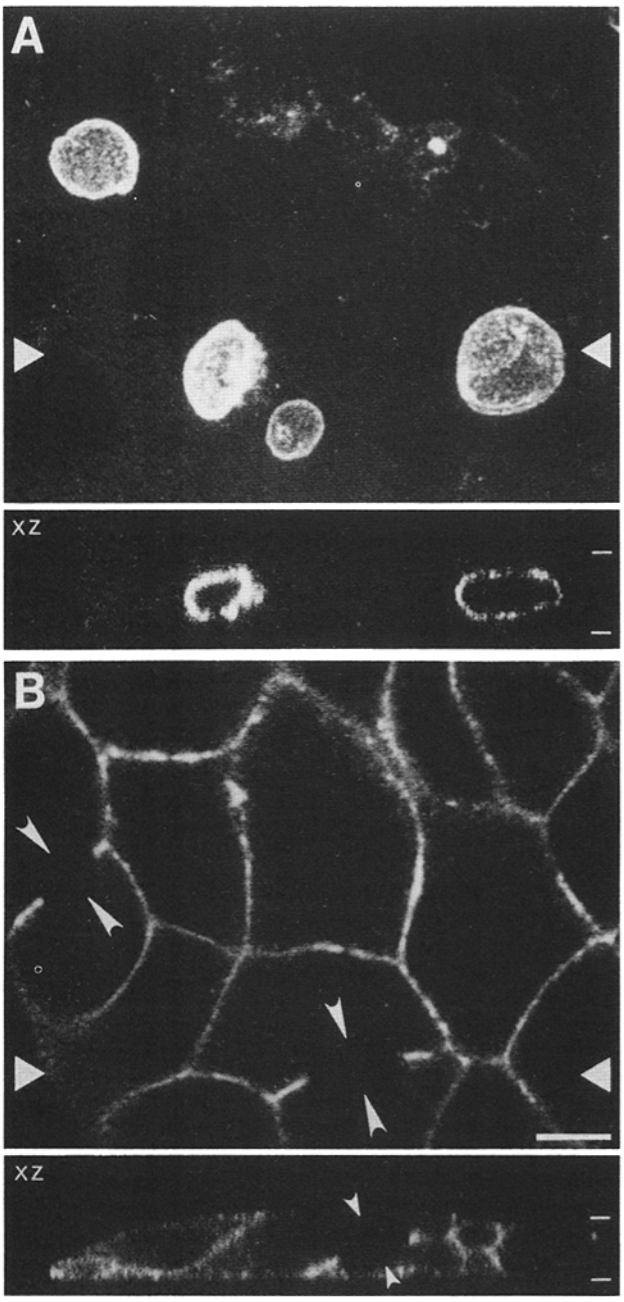

Figure 2. Apical and basolateral PM proteins show a polarized distribution in WIF-B cells. APN (*A*) and CE9 (*B*) were localized in WIF-B cells by LSCM with use of rabbit pAb followed by goat FITC-IgG (Pasteur Production). The upper panel of APN (*A*) shows a compiled z series taken in 1 μm steps and the upper panel of CE9 (*B*) a single 1 μm optical x-y section taken ~7 μm from the bottom of the cells. The lower panels show 1 μm optical x–z sections through the cells at the location indicated by triangles in the x–y images; dashes mark the top and bottom of the cell layer. APN (*A*) is located at the membrane of all four BC structures. The basolateral marker CE9 (*B*) is excluded from the two visible BC (*arrowheads*). Note the partially overlapping growth of cells and the sequestered location of BC between adjacent cells in the x–z section (*B*). Bar, 10 μm.

reconstruction (Fig. 2). That is, they were sequestered away from both the attached and free surfaces of the cells.

We determined the extent to which two PM proteins localized with each other by double immunofluorescence and quantification (Table I). Combinations of apical PM proteins were found together in 94 to 99% of the translucent structures. The basolateral marker CE9 was absent from 96 to 99% of the structures labeled by an apical marker and HA321 was never found together with apical markers. In the few cases where CE9 co-localized with apical proteins, the phase-lucent structures often appeared to be intracellular. There were also occasionally intracellular "vacuolar compartments" that contained only apical markers as have been described for other polarized cell lines (Vega-Salas et al., 1987; Le Bivic et al., 1988). Under optimal culture conditions, as judged by LSCM, the intracellular population accounted for about 10% of all translucent structures. We consider the intercellular population (~90%) equivalent to bile canaliculi and define these structures as BC.

Cytoskeletal Proteins and the Tight Junction–associated ZO-1 Show a Polarized Distribution

Actin Filaments and Microtubules. The arrangement of cytoskeletal elements in WIF-B cells was determined by conventional immunofluorescence microscopy. In cells treated with rhodamine-labeled phalloidin a thin but highly concentrated enveloping network of actin filaments was observed around the BC, together with a sparse network close to the basolateral membrane (Fig. 3 *B*). Microtubules, which were nearly always highly concentrated close to the BC, often radiated out from regions close to this membrane (Fig. 3 *C*). This arrangement was most obvious in flatter regions of the culture. Here, microtubules appeared to extend out towards both the basolateral membrane and the nucleus (Fig. 3 *C*). In thicker areas of the culture, the high abundance of microtubules prevented precise localization of their ends. To verify the spatial relationship of the cytoskeleton with the apical and basolateral PM domains, double-labeling experiments with antibodies to the cytoskeletal markers and to HA4 or HA321, respectively, were performed (data not shown).

Localization of γ-Tubulin. To determine the possible position of the microtubule organizing center, cells were double labeled with antibodies to both α- and γ-tubulin. In 90% of cells contributing to the formation of a BC, a variable number of γ-tubulin foci (range 1–9) were positioned close to the apical PM (Fig. 4 *B*). Rarely (<1% of the BC), γ-tubulin formed a discontinuous ring near BC (data not shown). In one-third of all BC examined, γ-tubulin foci were positioned near the apical domain in one of the participating cells only. Although 10% of the BC had no detectable γ-tubulin nearby, microtubules were still highly concentrated in this region (data not shown). There was no obvious emanation of microtubules from γ-tubulin foci under steady state conditions, although after either cold- or nocodazole-induced depolymerization, initiation of microtubule polymerization was observed in areas containing γ-tubulin (data not shown).

Localization of the Tight Junction Protein ZO-1. Tight junctions are marked by the membrane-associated protein ZO-1 (reviewed by Schneeberger and Lynch, 1992). The

*Table I. Apical Proteins Co-localize at BC of WIF-B Cells**

	DPPIV‡ (ap)	HA4‡ (ap)	APN‡ (ap)	5'NT‡ (ap)	CE9‡ (bl)	HA321‡ (bl)
	(percent of translucent structures double labeled)					
DPPIV§ (ap)	–	99	94	98	2	0
HA4§ (ap)	98	–	97	95	4	0
CE9§ (bl)	3	2	1	3	–	0‖
ZO-1§ (tj)	96	96	95	96	0	0

ap, apical; bl, basolateral; tj, tight junctional.
* WIF-B cells grown on coverslips were fixed, permeabilized, and stained for double immunofluorescence as described in Materials and Methods. At least 200 BC were examined for each pair-wise comparison.
‡ First PM protein visualized by rabbit pAb followed by swine rhodamine-IgG.
§ Second PM protein visualized by guinea pig pAbs (DPPIV and CE9), or rat mAb (ZO-1) followed by goat FITC-IgG (Sigma), or mouse mAb (HA4) followed by goat FITC-IgG (Jackson).
‖ HA321 and CE9 co-localized at the basolateral PM, but were never found together in translucent structures.

three-dimensional appearance of this protein in WIF-B cells was determined by LSCM (Fig. 5). The apical domain was labeled in the same cells by using an antibody to HA4. To visualize the spherical BC architecture (Fig. 5 *C*), the image of a combined z series for ZO-1 (Fig. 5 *A*) was merged with a single optical x-y section for HA4 (Fig. 5 *B*). ZO-1 was localized in beltlike structures surrounding BC at the contact sites of adjacent cells. Most of the BC (86%) were formed by two cells and one belt was located between the two cells. The other BC had two or more connected belts around them, indicating that three or more cells were participating to form a BC (Fig. 5 *A, inset*). We quantified the extent to which ZO-1 co-localized with different PM markers by double immunofluorescence (Table I): 95–96% of the translucent structures that were positive for apical PM proteins were also positive for ZO-1. The small fraction that contained apical markers but showed no staining for ZO-1 appeared to be intracellular structures (Fig. 5). Conversely, the basolateral markers CE9 and HA321 never co-localized with ZO-1, suggesting the presence of a diffusion barrier at the domain boundary marked by this tight junction protein.

A Diffusion Barrier to Sphingolipids Is Present between the Apical and Basolateral PM Domains

Fluorescent Sphingomyelin at the Basolateral PM Does Not Diffuse to the Apical PM. The presence of a diffusion barrier to lipids in the PM of WIF-B cells was first assessed using an exogenously added fluorescent sphingomyelin analog, C_5-DMB-SM. Cells were incubated with C_5-DMB-SM at 2°C, washed, further incubated either in the presence or absence of back-exchange medium at 10°C, and then observed by LSCM. After incubation with C_5-DMB-SM the basolateral PM domain was intensely fluorescent in all cells examined while the apical PM domain of most cells appeared to be unlabeled (Fig. 6 *A*). Similar results were also obtained after cells were incubated as above with other fluorescent analogs of sphingomyelin, or with a glycolipid analog, C_5-DMB-galactosylceramide (data not shown). Treatment of C_5-DMB-SM–labeled cells with back-exchange medium completely removed fluorescence at the PM (Fig. 6 *B*), suggesting that the fluorescent lipid was associated with the outer leaflet of the membrane bilayer (Koval and Pagano, 1990; van Meer et al., 1987).

Although the apical PM domain of the majority of cells was unlabeled (Fig. 7 *A*), a small amount of fluorescence was seen in ~20% of the cells (Fig. 7, *B* and *C*). In these cells, the tightness of the diffusion barrier might have been temporarily altered, allowing diffusion of sphingolipid from the basolateral to the apical PM domain. It is also possible that fluorescent sphingolipid gained direct access to the apical PM domain via a paracellular route. In either event, the percentage of BC labeled with exogenously applied fluorescent sphingomyelin was relatively small.

Fluorescent Sphingomyelin at the Apical PM Does Not Diffuse to the Basolateral PM. To learn whether sphingolipids present at the apical PM domain of WIF-B are restricted to that domain by a diffusion barrier, both PM domains were first labeled by delivery of fluorescent sphingomyelin along the secretory pathway following its de novo synthesis from a fluorescent ceramide analog (reviewed in Pagano, 1990; Rosenwald and Pagano, 1993). Cells were then incubated with back-exchange medium. If a diffusion barrier is present, only the basolateral PM should contact the back-exchange medium and only its fluorescence should be removed. In the absence of a diffusion barrier, back-exchange should remove fluorescence from both plasma membrane domains.

WIF-B cells were incubated with C_5-DMB-Cer at 2°C, washed, and further incubated at 20°C to allow the fluorescent ceramide to accumulate at the Golgi apparatus and be metabolized (Lipsky and Pagano, 1983, 1985; van Meer et al., 1987; van't Hof and van Meer, 1990). The cells were then washed and incubated in back-exchange medium at 10°C to remove any fluorescent sphingolipid present at the PM (Fig. 8 *A*). Cells treated in this manner demonstrated intense fluorescence at the Golgi apparatus, diffuse cytoplasmic fluorescence, and an absence of fluorescence at either PM domain. Quantitative analysis of lipids extracted from cells treated in this manner revealed that ~67% of the C_5-DMB-Cer was converted to C_5-DMB-SM. When cells treated as in Fig. 8 *A* were further incubated for 30 min at 37°C, prominent fluorescence at both the apical and basolateral PM domains was seen (Fig. 8 *B*). However, when cells treated as in Fig. 8 *B* were subsequently incubated with back-exchange medium at 10°C, prominent fluorescence was observed at the apical (but not basolateral) PM domain (Fig. 8 *C*). These experiments demonstrate the presence of a diffusion barrier to fluorescent sphingomyelin at the boundary between apical and basolateral PM domains.

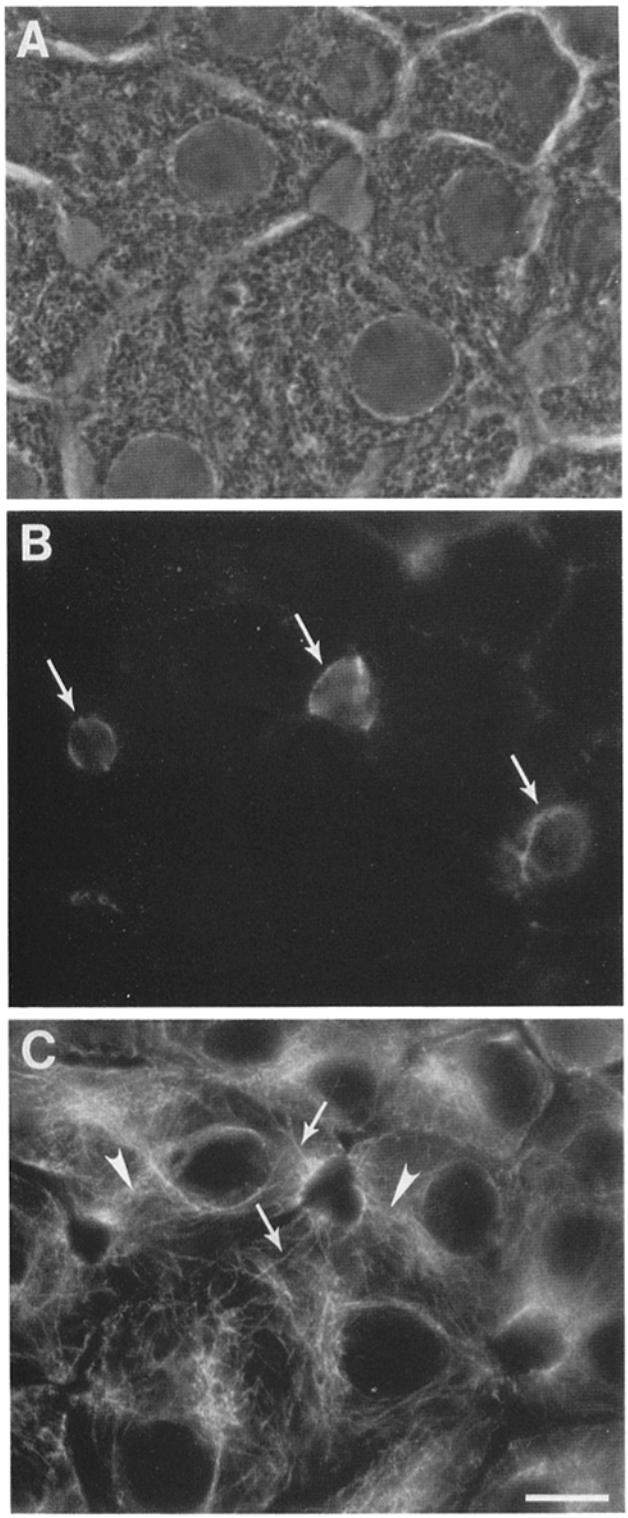

Figure 3. Actin filaments and microtubules are associated with the BC of WIF-B cells. WIF-B cells (phase image shown in *A*) were double labeled for actin (*B*) and microtubules (*C*). Actin filaments were visualized with rhodamine-conjugated phalloidin and microtubules were stained with mouse anti-α-tubulin mAb, followed by horse FITC-IgG. Actin filaments (*B*) form a thin enveloping network around BC (*arrows*). Microtubules (*C*) radiate out from regions close to the BC membrane; some appear to pass towards the basolateral membrane (*arrows*), while others are directed towards the nuclear region (*arrowheads*). Bar, 10 μm.

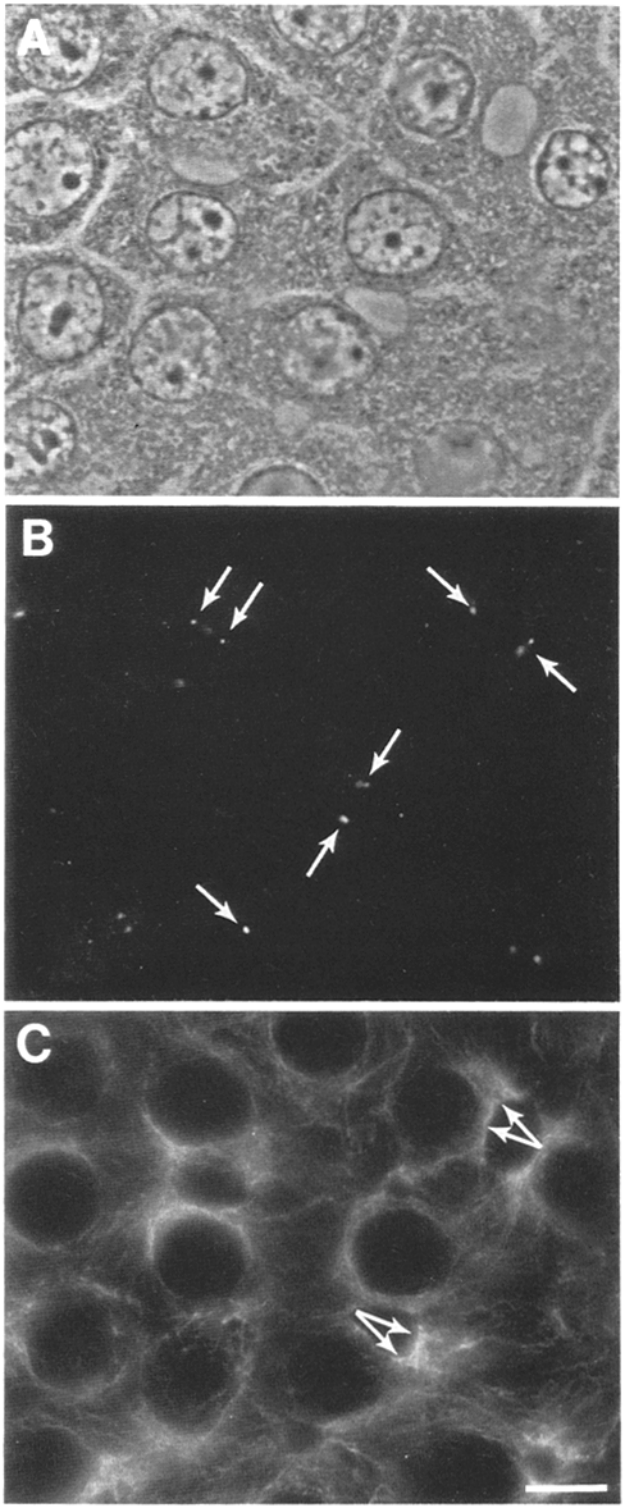

Figure 4. Discrete foci of γ-tubulin are located close to BC. WIF-B cells (phase image shown in *A*) were double labeled for γ-tubulin (*B*) and microtubules (*C*). γ-Tubulin was stained with rabbit pAb, followed by goat FITC-IgG; microtubules were labeled with mouse anti-α-tubulin mAb, followed by goat TRITC-IgG. Discrete foci of γ-tubulin (*B*) are present close to the membrane of most BC (*arrows*). Microtubules (*C*) are not obviously associated with γ-tubulin and radiate out from regions close to the BC membrane irrespective of the location of γ-tubulin (*arrows*). Bar, 10 μm.

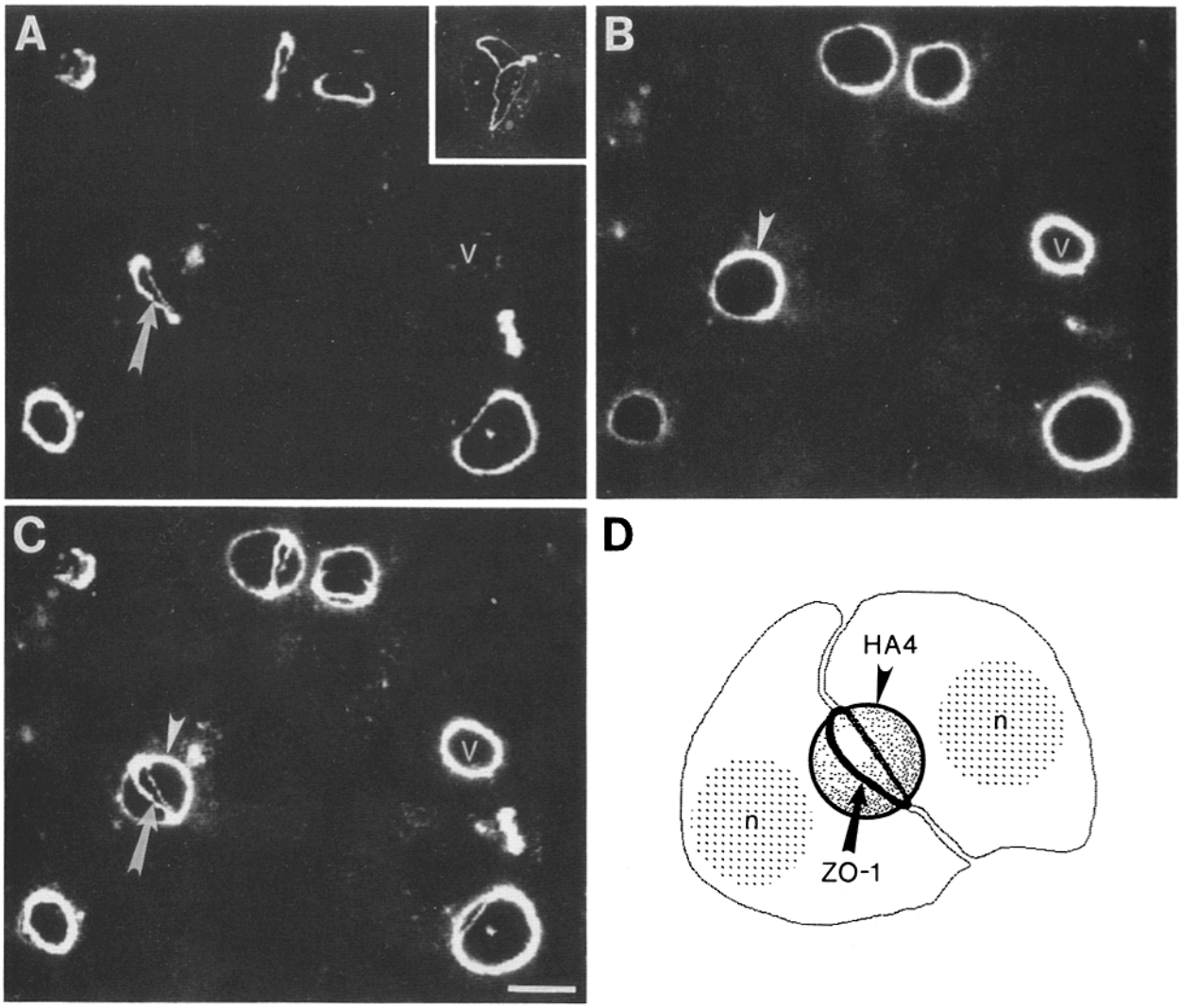

Figure 5. ZO-1 marks the borders between apical and basolateral domains. WIF-B cells were double labeled for the tight junction–associated protein ZO-1 (*A* and *C*) and the apical marker HA4 (*B* and *C*). (*D*) Schematic drawing of the BC in *A–C* which is marked by an arrow and/or arrowhead (*n* = nucleus of adjacent cell). ZO-1 (*arrows*) was visualized with rat mAb followed by goat FITC-IgG (Kirkegaard and Perry), and HA4 (*arrowheads*) was stained with rabbit pAb followed by goat Texas red-IgG (Jackson). The image of ZO-1 (*A*) is a compiled z-series taken in 1 μm steps, and that of HA4 (*B*) is a 1-μm optical x–y section. Both images (*A* and *B*) were merged to generate the image in *C* to illustrate the three-dimensional BC architecture. The beltlike presence of ZO-1 around BC between the participating cells suggests the existence of tight-junctional structures separating apical and basolateral domains. In *B* and *C* one can see an intracellular "vacuolar compartment" (*v*) which is positive for HA4 but has no ZO-1 staining (*A* and *C*). The inset in *A* shows an example of three cells forming a BC with two connected ZO-1 belts around the BC, a phenomenon observed in 12% of all BC (*n* = 200). In a few cases (2%), even three or more ZO-1 belts were visible (% of total BC, *n* = 200). Bar, 10 μm.

The Boundary between the Apical and Basolateral Domains Shows Selectivity to the Diffusion of Soluble Molecules

Diffusion of FITC-labeled Dextrans. We next explored the properties of the boundary between apical and basolateral domains in living WIF-B cells using soluble molecules. Confluent cells were incubated with FITC-dextrans of 4,400, 35,600, and 71,200 D for 5 to 10 min at 37°C or for 60 min on ice, washed quickly, and observed within 10 min. Since intracellular staining was not observed under these conditions (data not shown), the dextrans served as extracellular reporter molecules for the diffusion selectivity of the domain boundary. At 37°C, there was substantial staining of BC with dextrans of all sizes. This was most pronounced for the 4,400-D dextran which labeled 78% of the BC (Fig. 9, *A* and *B*). The labeling diminished as the size of the dextrans increased; the largest dextran tested (71,000 D) labeled only 13% of the BC (Fig. 9 *B*). Interestingly, at low temperatures the BC were less accessible to dextrans of all sizes. Only 36% of the BC contained label when cells were incubated with the 4,400-D dextran on ice, even though the incubation time was extended to 60 min. The fraction of labeled BC diminished to <5% with the largest probe used (Fig. 9 *B*). This indicates that the boundary between the apical and basolateral domains is selective to the diffusion of soluble molecules and that the selectivity is temperature dependent. We did not observe significant differences whether incubations were carried out in the presence or absence of Ca^{2+} (see Discussion).

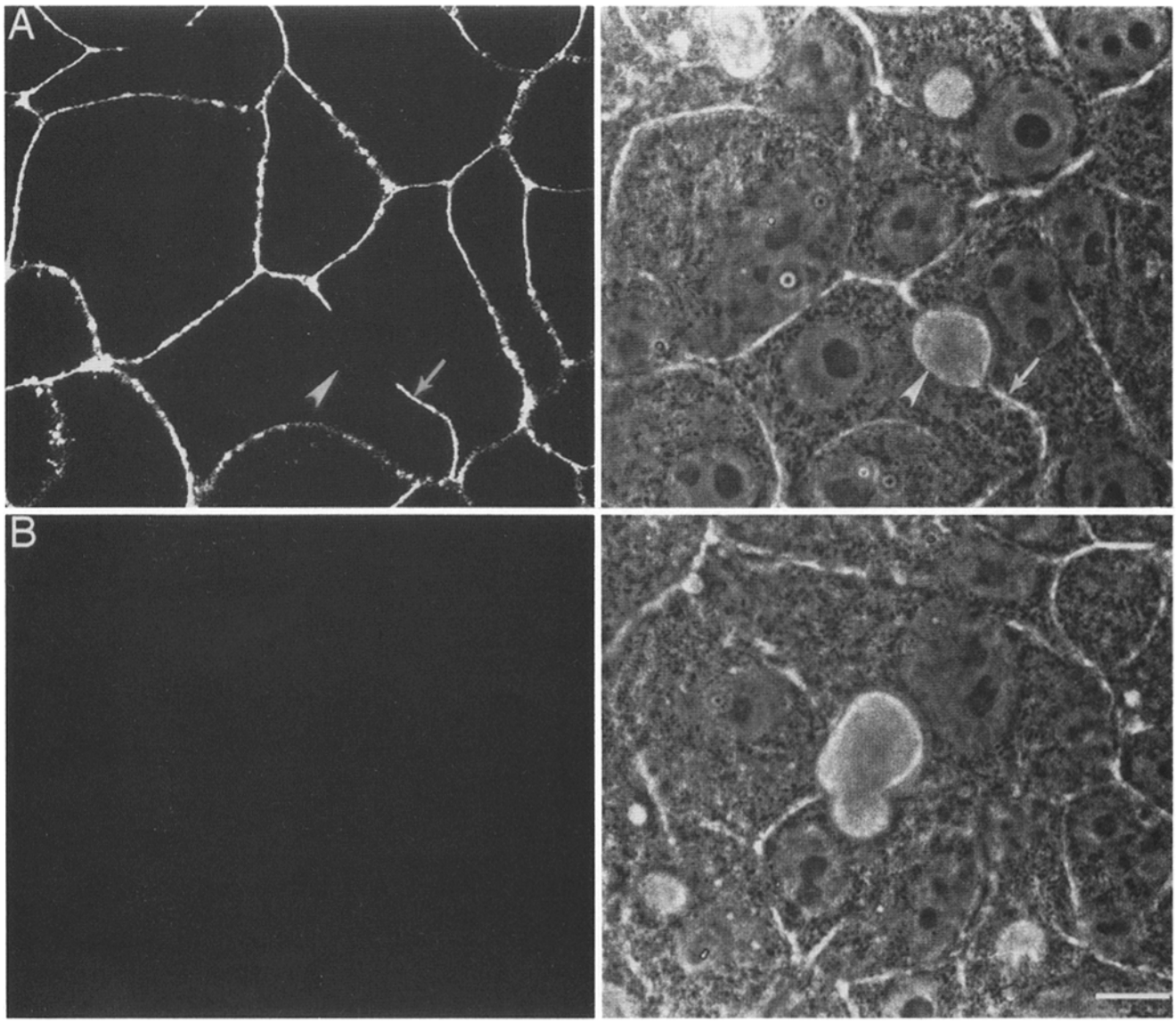

Figure 6. Exogenously applied fluorescent sphingomyelin integrates into the basolateral PM. Cells were incubated with 5 μM C_5-DMB-SM/DF-BSA for 30 min at 2°C, washed, and photographed immediately (*A*), or, further incubated with 5% DF-BSA ("back-exchanged") to remove fluorescent lipid at the plasma membrane before photography (*B*). The phase-contrast image corresponding to each fluorescence micrograph is shown at the right. Arrows and arrowheads show the location of the basolateral surface and BC, respectively. LSCM scans were performed under identical conditions and all confocal micrographs were exposed and printed identically. Bar, 10 μm.

Accessibility of the BC for Biotin and Streptavidin. Membrane-impermeable derivatives of biotin are commonly used as covalent cell surface labels in living cultures of polarized cells (Sargiacomo et al., 1989; Rodriguez-Boulan, 1989). In monolayers of simple epithelial cells, exogenously applied biotin does not penetrate tight junctions, making it a suitable domain-specific probe (Sargiacomo et al., 1989). We labeled confluent WIF-B cultures with sNHS-LC-biotin (557 D) for 30 min at 4°C, and then fixed the cells and visualized biotinylated PM proteins with FITC-streptavidin. All basolateral cell surfaces and ~80% of the BC surfaces were stained (Fig. 10 *A*). The level of labeling intensity at the BC relative to the basolateral signal varied to some degree, depending on the buffer system used (data not shown). Raising the pH from 7.5 to 9.0 resulted in much brighter overall staining. However, varying the temperature, pH, or incubation time did not significantly change the total number of labeled BC. In ~20% of the total population the domain boundary prevented paracellular diffusion of biotin.

When biotinylation of the cells was followed by an incubation with unconjugated streptavidin at 4°C before fixation and detection with FITC-streptavidin, basolateral domains were no longer positive (Fig. 10 *B*). In contrast, apical membrane domains were stained with the fluorescent probe as before, confirming that large molecules, such as streptavidin, are excluded from the BC of living WIF-B cells at low temperatures.

Discussion

We have evaluated the WIF-B cell line as a potential candidate for in vitro studies of vectorial membrane traffic in polar-

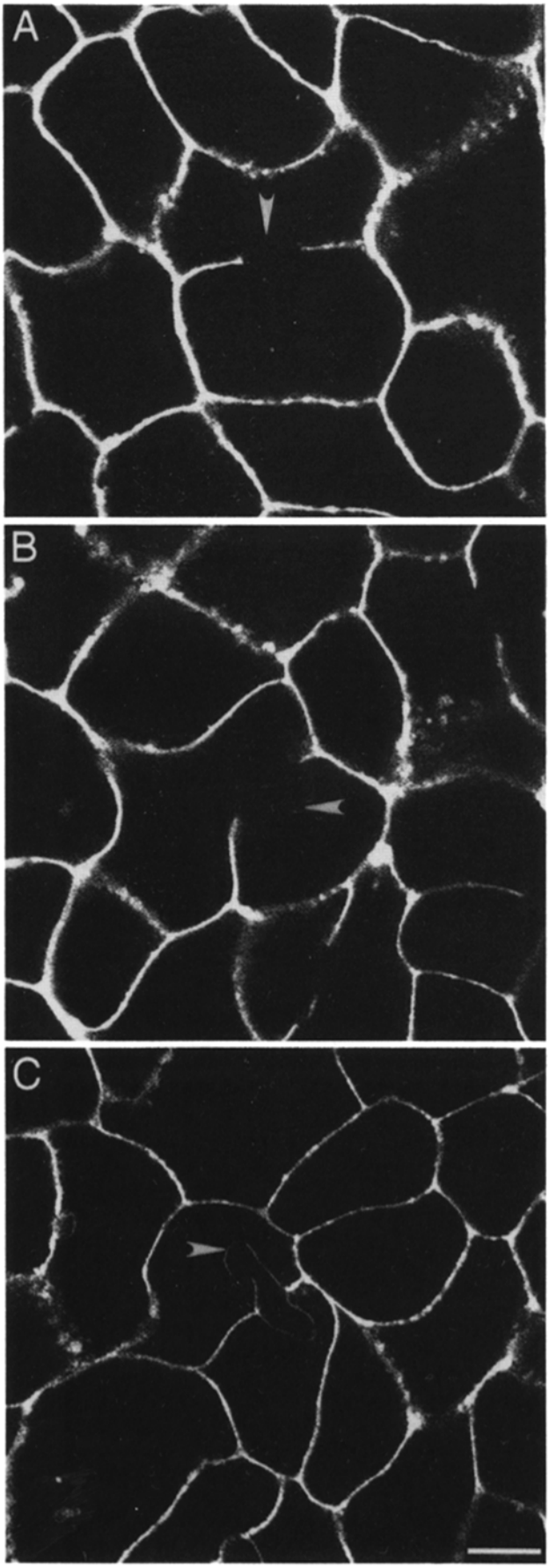

ized hepatocytes. We first confirmed and extended the observations made by Cassio et al. (1991) of the WIF 12-1 cells, the WIF-B antecedent. Under optimal culture conditions, the WIF-B cells maintain many of the hallmarks of the polarized hepatocyte in situ. PM proteins that are restricted to either the apical (bile canalicular) or basolateral domain in situ show similar steady-state distributions in WIF-B cells. Excretion of organic anions into the spherical BC further indicates that these structures are the functional equivalent of bile canaliculi in vivo. ZO-1 localizes to the boundaries between BC and basolateral domains, indicating the presence of tight junctions. We then explored two areas where much less is known in vivo at the individual cell level: the architecture of the cytoskeleton and the "fence and gate" properties of the domain boundary in living cells. Microtubule and actin-based filaments show a preferential association with the BC structures in WIF-B cells. The diffusion of membrane sphingolipids is constrained by the domain boundary marked by ZO-1 in WIF-B cells. Finally, small but not large soluble molecules have reasonably free access to the BC space and membrane, allowing the modified use of well-characterized vectorial labels in these cells. Consequently, we think the WIF-B cells provide a valid in vitro model for polarized hepatocytes.

Polarized Organization of WIF-B Cells

The WIF-B cells present a different polarized phenotype from that of either simple columnar epithelial cells or hepatocytes in situ. In monolayer culture on tissue culture plastic, the apical domain is hidden between adjacent cells and sealed off from direct experimental access. Furthermore, the individual apical structures, which we term "BC," do not form anastomosing networks of canals as in vivo. Nevertheless, they are the functional equivalent of BC by all criteria we applied. The ability of WIF-B cells to accumulate fluorescein and a fluorescent derivative of the bile acid glycocholate in the BC suggests the existence of functional hepatic transporter systems like the apical multispecific organic anion transporter (Elferink et al., 1990; Kitamura et al., 1990; Ishikawa et al., 1990) and bile acid transporter(s) (reviewed by Nathanson and Boyer, 1991). The immunofluorescence studies show that the distribution of known apical (APN, DPPIV, HA4, and 5'NT) and basolateral PM domain markers (CE9 and HA321) closely resembles their localization in situ (Bartles et al., 1990; Scott and Hubbard, 1992; Barr and Hubbard, 1993; Luzio et al., 1986). In vivo and in vitro the glycosylphosphatidylinositol-linked protein 5'NT

Figure 7. Exogenously applied fluorescent sphingomyelin is excluded from apical PM domains. Cells were incubated with 5 μM C_5-DMB-SM/DF-BSA for 30 min at 2°C, washed, and photographed. BC (*arrowheads*), initially identified by phase microscopy, were classified as (*A*) unlabeled (80.6 $\pm$ 2.0%), (*B*) partially labeled (14.1 $\pm$ 2.1%), or (*C*) fully labeled (5.5 $\pm$ 1.6%) during observation under epifluorescence illumination (data represent % of total BC [mean $\pm$ S.D.; n = 2322]). LSCM scans were performed under identical conditions and all micrographs were exposed and printed identically. Bar, 10 μm.

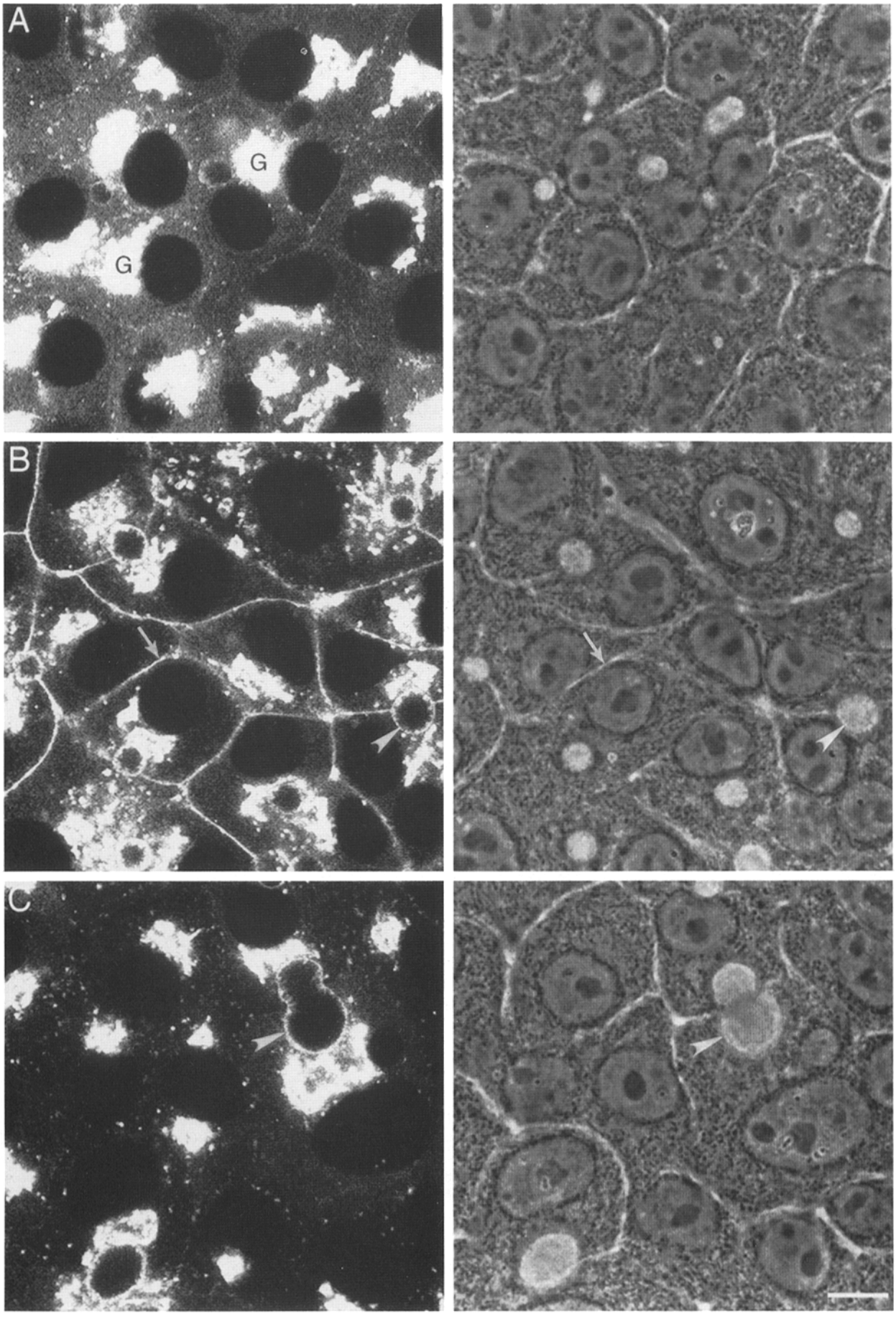
A
G
G
B
C

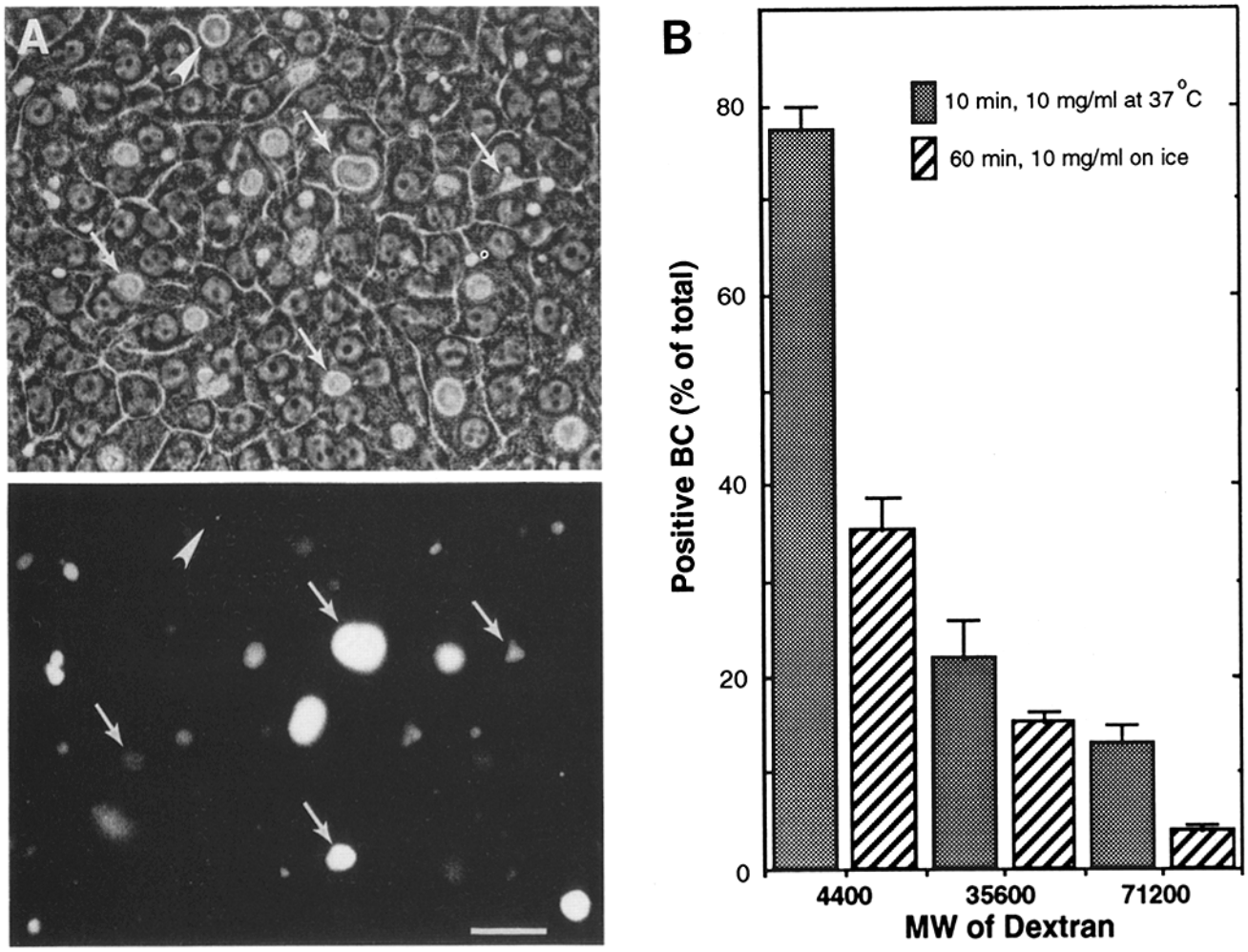

Figure 9. The paracellular diffusion of FITC-dextrans across the domain-boundary is size and temperature dependent. Confluent cells were incubated with 10 mg/ml FITC-dextrans of the indicated molecular weight at 37°C for 10 min or on ice for 60 min, washed, and immediately observed at a fluorescence microscope. (*A*) WIF-B cell culture after incubation with a 4,400-D dextran for 10 min at 37°C under phase contrast (*top*) and epifluorescence illumination (*bottom*); arrows point to labeled BC, the arrowhead indicates an unlabeled BC. (*B*) FITC-dextran positive spaces were counted and expressed as percent of translucent areas observed at phase contrast. Bar, 25 μm.

seems to be less highly polarized than the other PM markers, since a weak label is also seen in the basolateral domain (Luzio et al., 1986). The restriction to one or the other PM domain of all integral proteins studied implies the presence of a barrier preventing intermixing of proteins between domains (Pisam and Ripoche, 1976; Edidin, 1992) and the existence of mechanisms to deliver and/or retain them in the correct membrane domain (reviewed by Schneeberger and Lynch, 1992).

The polarized distribution of different domain markers correlates with the localization of ZO-1 in beltlike structures around the BC of WIF-B cells. The peripheral membrane protein ZO-1 is generally regarded as a good marker for the presence of tight junctions (reviewed in Citi, 1993). It was originally shown to be associated with hepatic tight junctions in mouse liver (Stevenson et al., 1986; Anderson et al., 1988). In recent EM studies, some ZO-1 staining was also found in the region of the adherens junctions in rat hepatocytes (Itoh et al., 1993), a result that might be related to the less-developed character of liver tight junctions as compared to other epithelia. However, its concentration at the expected site of the junctional complex in WIF-B cells suggests the

Figure 8. Fluorescent sphingomyelin present at the apical PM does not diffuse into the basolateral domain. Cells were incubated with 5 μM C_5-DMB-Cer/DF-BSA for 30 min at 2°C, washed, incubated in HSFM for 2 h at 20°C, washed, and subsequently back-exchanged with 5% DF-BSA at 10°C to remove fluorescent lipid present at the PM (note prominent labeling of the Golgi apparatus [*G*]) (*A*). Cells were then further incubated for 60 min at 37°C, washed, and photographed immediately (*B*), or, subsequently back-exchanged with 5% DF-BSA (*C*). Note that both the basolateral (*arrow*) and the apical (*arrowhead*) PM domains are labeled in *B*, while only the apical domain (*arrowhead*) is labeled in *C*. The phase-contrast image corresponding to each fluorescence micrograph is shown at the right. LSCM scans were performed under identical conditions and all confocal micrographs were exposed and printed identically. Bar, 10 μm.

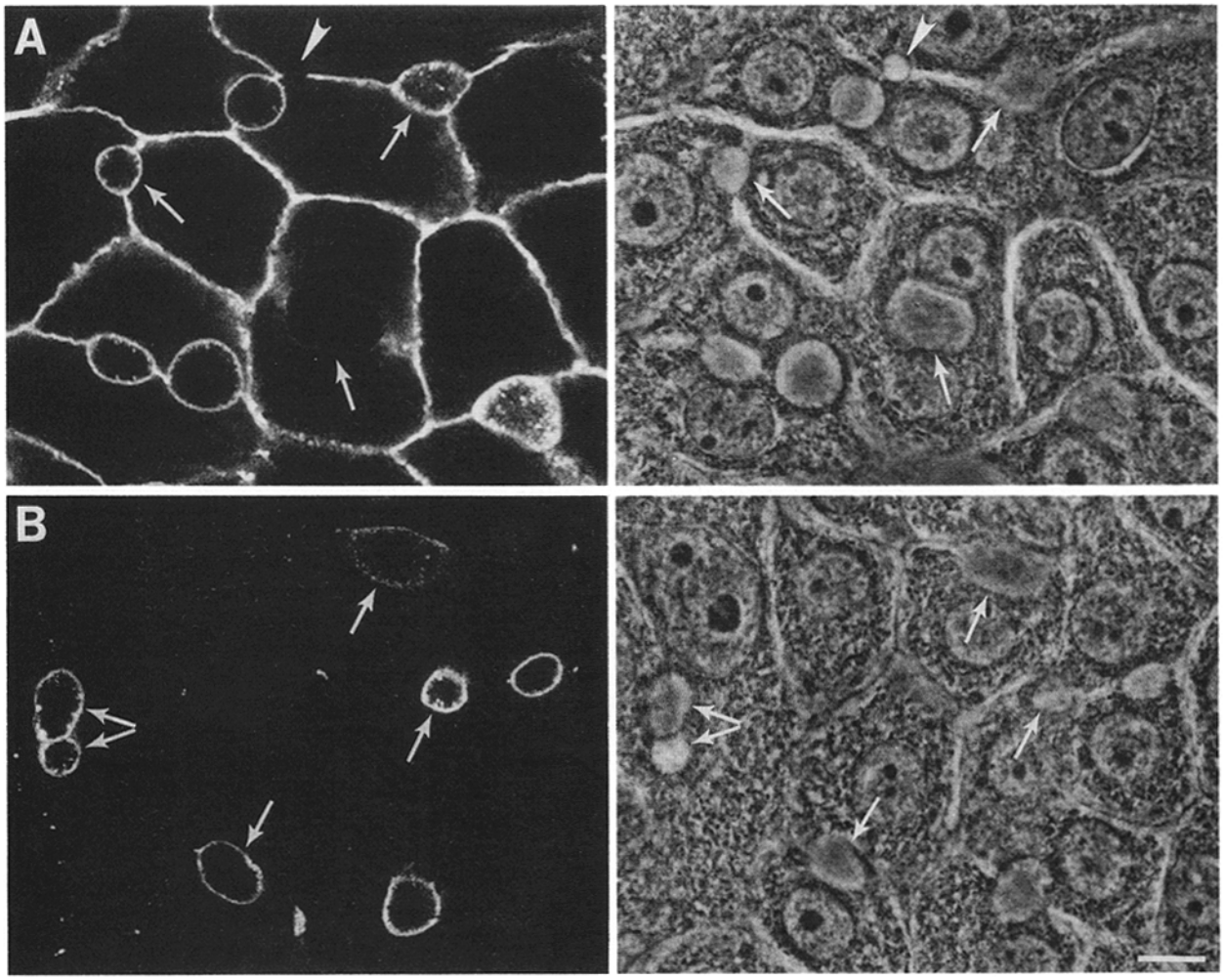

Figure 10. Apical domains are accessible to biotin but exclude streptavidin. Confluent WIF-B cells were biotinylated at the cell surface with sNHS-LC-biotin in borate buffer, pH 9, at 4°C. Cells were then (*A*) fixed and incubated with FITC-streptavidin or (*B*) incubated with unconjugated streptavidin before fixation and detection with FITC-streptavidin. Basolateral domains as well as the membranes of most BC (*arrows*) are efficiently labeled in the absence of unconjugated streptavidin (*A*). When the living cells were incubated with unconjugated streptavidin after biotinylation, basolateral surfaces were masked for later binding of FITC–streptavidin, resulting in specific labeling of apical domains (*B*). About 20% of the BC are not accessible even to biotin under either condition (arrowhead). With the borate buffer system ~60% of the BC are at least as brightly labeled as the basolateral domain, whereas ~20% are less brightly labeled. The phase-contrast image corresponding to each fluorescence micrograph is shown at the right. LSCM scans were performed under identical conditions and all confocal micrographs were exposed and printed identically. Bar, 10 μm.

presence of tight junctions, an assumption supported by EM studies in WIF12-1 (Cassio et al., 1991) and WIF-B cells (data not shown).

In addition to the polarized distribution of PM proteins, cytoskeletal elements also displayed polarity in WIF-B cells. Actin filaments were predominantly concentrated in a thin network around the BC membrane and microtubules radiated from areas close to the BC. The actin distribution resembles that of actin filaments around bile canaliculi in hepatocytes in vivo, which has been described as a "pericanalicular web" (Oda et al., 1974; Ishii et al., 1991). It is possible that these actin filaments have a functional role in the periodic contractions of BC that have been observed in WIF12-1 cells (Cassio et al., 1991). Several studies provide evidence that active bile canalicular contractions involving pericanalicular actin have a physiological role in bile flow (Phillips et al., 1983; Watanabe et al., 1991; Tsukuda and Phillips, 1993). However, the contractile properties of BC in WIF-B cells have not yet been studied.

The arrangement of microtubules in hepatocytes in vivo has been partially elucidated (reviewed by French et al., 1987). Bundles of microtubules are detectable, both in the perinuclear area, and running parallel to the cell cortex. In primary hepatocytes, disruption of microtubules prevents development of fully polarized and functional BC (Durand-Schneider et al., 1991). Several reports show that apical transport of PM proteins in simple epithelia is facilitated by microtubules (Rindler et al., 1987; Acheler et al., 1989; Matter et al., 1990; Hunziker et al., 1990; Gilbert et al., 1991). Microtubules in simple polarized epithelial cell models have been well studied. Bundles of microtubules running between the apical and basal domains are oriented with their minus end towards the apical surface in MDCK cells (Bacallao et al., 1989) and Caco-2 cells (Meads, T., and T.

Schroer, unpublished observations). Centrosomes in MDCK cells are localized near the apical pole (Buendia et al., 1990). γ-Tubulin, a centrosomal component that plays an active role in microtubule nucleation (Stearns et al., 1991; Joshi et al., 1992), is often positioned close to the BC membrane in WIF-B cells, and microtubules nucleate from these regions after depolymerization (data not shown). It is thus tempting to speculate that microtubules in WIF-B cells are oriented with their minus end towards the apical domain, as in MDCK and Caco-2 cells, and that they play a role in polarized trafficking of proteins.

In the minority of WIF-B cells that were unpolarized, the distribution of microtubules was more symmetric, reminiscent of that in fibroblasts, and microtubules were concentrated around the nucleus. In the same cells, the localization of PM protein was not confined to discrete domains. Moreover, we saw no beltlike ZO-1 staining around BC (data not shown). These results emphasize that the fully polarized hepatocyte phenotype is a consequence of multiple vectorial functions acting in concert, the appearance of which seems to correlate with the existence of tight junctions.

Restricted Diffusion of Fluorescent Sphingolipids across the Domain Boundary

We have shown that exogenously applied fluorescent sphingomyelin analogs associated with the basolateral PM domain of WIF-B cells were excluded from the BC and could be readily removed by incubation with back-exchange medium. This domain-specific restriction was observed using several different sphingolipid analogs with different fluorescent fatty acid or head group moieties. Moreover, fluorescent sphingolipid synthesized de novo and delivered to the PM along the secretory pathway could be removed from the basolateral surface, but not from BC, by back-exchange. Taken together, these results provide strong evidence that the fluorescent sphingomyelin resided in the outer leaflet of the PM bilayer and that a barrier to diffusion of sphingolipids exists between the apical and basolateral PM domains.

It is likely that tight junctions provide the barrier to diffusion of lipids between WIF-B PM domains, as has previously been shown for MDCK, Caco-2, and other polarized epithelial cells in vitro (Dragsten et al., 1981; Spiegel et al., 1985; van Meer et al., 1987; van't Hof and van Meer, 1990). The observed restriction of fluorescent sphingolipids to WIF-B cell PM domains is consistent with the "fence" model of the tight junction (Dragsten et al., 1981; van Meer et al., 1986) wherein the tight junction serves as a barrier to diffusion between PM domains of lipids in the outer leaflet of the membrane bilayer. The tight junction "fence" functions to maintain compositional differences between PM domains in polarized cells. While we have not examined the lipid compositions of PM domains in WIF-B cells, these reportedly differ in hepatocytes (Higgins and Evans, 1978; reviewed in Koval and Pagano, 1991). The observation of a diffusion barrier to lipids between WIF-B cell PM domains is consistent with tight junctions having the same "fence" function in hepatocytes.

Selective Paracellular Diffusion through the Domain Boundary

A second function of tight junctions is as a "gate" that controls the paracellular movement of solutes across the epithelium, from blood to bile in liver (reviewed by Sellinger and Boyer, 1990). The "gate" and "fence" functions seem to be regulated by different factors and can be uncoupled (Mandel et al., 1993). WIF-B tight junctions are leaky at 37°C to molecules ≤35,600 D, but the accessibility of the BC decreases markedly with increasing molecular weight of the molecules and at lower temperatures. Although we cannot rule out that some fluorescent molecules reach the BC via transcytosis, the short incubation times (5–10 min) used gave no significant fluorescence inside of cells, although punctate spots were detectable at >30 min.

Under physiological conditions in vivo, transcytosis accounts for the appearance of large molecules (i.e., HRP-40,000 D) in bile (Lake et al., 1985). In contrast, paracellular diffusion of smaller molecules seems to be important for normal bile flow (reviewed by Sellinger and Boyer, 1990). However, the relative importance of the paracellular versus transcytotic routes cannot be assessed at the individual cell level in vivo as can be done in vitro. Since hepatic tight junctions are plastic structures, the permeability might vary among cells in the population. Nonetheless it is possible that the average tight junction permeability is higher in WIF-B cultures compared to that of hepatocytes in vivo. In this regard, it is curious that a small molecule such as fluorescein is retained in the BC for a prolonged period. It is consistent with the cation selectivity of leaky epithelia that this organic anion does not easily diffuse across the domain boundary of WIF-B cells (Bradley and Herz, 1978).

Our initial attempts to regulate the tight junctions of WIF-B cells have not been conclusive. Deprivation of extracellular calcium did not affect their permeability significantly, suggesting that the integrity of hepatic tight junctions is less calcium dependent than those of other epithelia. This view is consistent with observations in the perfused liver and in vivo (Katsuya et al., 1978; Stevenson and Goodenough, 1984). However, studies in the perfused rat liver and in hepatocyte couplets clearly show that hepatic tight junctions are regulated by the concentration of intracellular calcium concentration (Lowe et al., 1988; Nathanson et al., 1992). Protein kinase C seems to play a major role in the regulation, as in simple epithelia (reviewed by Schneeberger and Lynch, 1992). Preliminary results in WIF-B cells are consistent with this concept (data not shown).

Our long term goal is to understand the routes and mechanisms of membrane traffic in epithelial cells. To study protein trafficking in WIF-B cells at a biochemical level, domain-specific labeling methods are required. Although the sequestration of apical domains in WIF-B cultures represents a challenge not present in monolayers of MDCK or Caco-2 cells, one can take advantage of the observed "permselectivity" of the tight junctions. Since small biotin derivatives, like sNHS-LC-biotin, gain access to the vast majority of BC, conventional biotinylation techniques can be applied to label the entire cell surface. The PM domains can then be discriminated by exclusion of large molecules like streptavidin from the BC.

The results presented in this study show that the WIF-B cell line is a suitable in vitro model for the study of protein and lipid trafficking in polarized hepatocytes. We are particularly interested in transcytosis in hepatocytes, since it is the predominant if not exclusive pathway in these cells for deliv-

ery of material to the apical domain. With this model we can determine the relative importance of the direct and indirect routes for the delivery of lipids and PM proteins to the apical cell surface and elucidate mechanisms of basolateral-to-apical transcytosis, a microtubule-dependent process. Furthermore, this cell line provides a potential model system for the study of physiological phenomena, such as regulation of tight junctions, bile acid secretion, and constitutive secretion of plasma proteins and lipoproteins.

This work was supported by Deutsche Forschungsgemeinschaft grant Ih 14/1-1 to G. Ihrke, Association pour la Recherche sur le Cancer grant 6551 and Institut Curie grant 949 to D. Cassio, a grant to Centre National de la Recherche Scientifique (URA 1343), a National Institutes of Health Program Project grant DK 44375 to T. A. Schroer, R. E. Pagano, and A. L. Hubbard, and NATO travel grant to A. L. Hubbard and D. Cassio.

Received for publication 30 August 1993 and in revised form 7 October 1993.

References

Achler, C., D. Filmer, C. Merte, and D. Drenckhahn. 1989. Role of microtubules in polarized delivery of apical membrane proteins to the brush border of the intestinal epithelium. *J. Cell Biol.* 109:179–189.

Anderson, J. M., B. R. Stevenson, L. A. Jesaitis, D. A. Goodenough, and M. S. Mooseker. 1988. Characterization of ZO-1, a protein component of the tight junction from mouse liver and Madin-Darby Canine Kidney cells. *J. Cell Biol.* 106:1141–1149.

Bacallao, R., C. Antony, C. Dotti, E. Karsenti, E. H. K. Stelzer, and K. Simons. 1989. The subcellular organization of Madin-Darby Canine Kidney cells during the formation of a polarized epithelium. *J. Cell Biol.* 109: 2817–2832.

Bailyes, E. M., M. Soos, P. Jackson, A. C. Newby, K. Siddle, and J. P. Luzio. 1984. The existence and properties of two dimers of rat liver ecto-5′-nucleotidase. *Biochem. J.* 221:369–377.

Barr, V. A., and A. L. Hubbard. 1993. Newly synthesized hepatocyte plasma membrane proteins are transported in transcytotic vesicles in the bile duct-ligated rat. *Gastroenterology.* 105:554–571.

Bartles, J. R., and A. L. Hubbard. 1990. Biogenesis of the rat hepatocyte plasma membrane. *Methods Enzymol.* 191:825–841.

Bartles, J. R., L. T. Braiterman, and A. L. Hubbard. 1985*a*. Biochemical characterization of domain-specific glycoproteins of the rat hepatocyte plasma membrane. *J. Biol. Chem.* 260:12792–12802.

Bartles, J. R., L. T. Braiterman, and A. L. Hubbard. 1985*b*. Endogenous and exogenous domain markers of the rat hepatocyte plasma membrane. *J. Cell Biol.* 100:1126–1138.

Bartles, J. R., H. M. Feracci, B. Stieger, and A. L. Hubbard. 1987. Biogenesis of the rat hepatocyte plasma membrane in vivo: comparison of the pathways taken by apical and basolateral proteins using subcellular fractionation. *J. Cell Biol.* 105:1241–1251.

Bhathal, P. S., and G. S. Christie. 1969. Intravital fluorescence microscopy of the terminal and subterminal portions of the biliary tree of normal guinea pigs and rats. *Lab. Invest.* 20:472–479.

Bradley, S. E., and R. Herz. 1978. Permselectivity of biliary canalicular membrane in rats: clearance probe analysis. *Am. J. Physiol.* 235:E570–E576.

Buendia, B., M.-H. Bre, G. Griffiths, and E. Karsenti. 1990. Cytoskeletal control of centrioles movement during the establishment of polarity in Madin-Darby Canine Kidney cells. *J. Cell Biol.* 110:1123–1135.

Cassio, D., C. Hamon-Benais, M. Guerin, and O. Lecoq. 1991. Hybrid cell lines constitute a potential reservoir of polarized cells: isolation and study of highly differentiated hepatoma-derived hybrid cells able to form functional bile canaliculi in vitro. *J. Cell Biol.* 115:1397–1408.

Chiu, J.-H., C.-P. Hu, W.-Y. Lui, S. J. Lo, and C. Chang. 1990. The formation of bile canaliculi in human hepatoma cell lines. *Hepatology.* 11:834–842.

Citi, S. 1993. The molecular organization of tight junctions. *J. Cell Biol.* 121:485–489.

Coon, H. G., and M. C. Weiss. 1969. A quantitative comparison of formation of spontaneous and virus-produced viable hybrids. *Proc. Natl. Acad. Sci. USA.* 62:852–859.

Dragsten, P. R., R. Blumental, and J. S. Handler. 1981. Membrane asymmetry in epithelia: is the tight junction a barrier to diffusion in the plasma membrane? *Nature (Lond.).* 294:718–722.

Durand-Schneider, A.-M., J.-C. Bouanga, G. Feldmann, and M. Maurice. 1991. Microtubule disruption interferes with the structural and functional integrity of the apical pole in primary cultures of rat hepatocytes. *Eur. J. Cell Biol.* 56:260–268.

Edidin, M. 1992. Patches, posts and fences: proteins and plasma membrane domains. *Trends Cell Biol.* 2:376–380.

Elferink, R. P. J. O., R. Ottenhoff, W. G. M. Liefting, B. Schoemaker, A. K. Groen, and P. L. M. Jansen. 1990. ATP-dependent efflux of GSSG and GS-conjugate from isolated rat hepatocytes. *Am. J. Physiol.* 258:G699–G706.

French, S. W., T. Okanoue, S. H. H. Swierenga, and N. Marceau. 1987. The cytoskeleton of hepatocytes in health and disease. *In* Pathogenesis of liver diseases. E. Farber, M. J. Phillips, and N. Kaufman, editors. Williams and Wilkins, Baltimore, MD. 95–112.

Gilbert, T., A. Le Bivic, A. Quaroni, and E. Rodriguez-Boulan. 1991. Microtubular organization and its involvement in the biogenetic pathways of plasma membrane proteins in Caco-2 intestinal epithelial cells. *J. Cell Biol.* 113:275–288.

Hanzon, V. 1952. Liver cell secretion under normal and pathologic conditions studied by fluorescence microscopy on living rats. *Acta Physiol. Scand.* 28 (Suppl. 101):5–268.

Higgins, J. A., and W. H. Evans. 1978. Transverse organization of phospholipids across the bilayer of plasma-membrane subfractions of rat hepatocytes. *Biochem. J.* 174:563–567.

Hoppe, C. A., T. P. Connolly, and A. L. Hubbard. 1985. Transcellular transport of polymeric IgA in the rat hepatocyte: biochemical and morphological characterization of the transport pathway. *J. Cell Biol.* 101:2113–2123.

Hubbard, A. L., J. R. Bartles, and L. T. Braiterman. 1985. Identification of rat hepatocyte plasma membrane proteins using monoclonal antibodies. *J. Cell Biol.* 100:1115–1125.

Hunziker, W., P. Male, and I. Mellman. 1990. Differential microtubule requirements for transcytosis in MDCK cells. *EMBO (Eur. Mol. Biol. Organ.) J.* 9:3515–3525.

Ishii, M., H. Washioka, A. Tonosaki, and T. Toyota. 1991. Regional orientation of actin filaments in the pericanalicular cytoplasm of rat hepatocytes. *Gastroenterology.* 101:1663–1672.

Ishikawa, T., M. Muller, C. Klunemann, T. Schaub, and D. Keppler. 1990. ATP-dependent primary active transport of cysteinyl leukotrienes across liver canalicular membrane. Role of the ATP-dependent transport system for glutathione S-conjugates. *J. Biol. Chem.* 265:19279–19286.

Itoh, M., A. Nagafuchi, S. Yonemura, T. Kitani-Yasuda, S. Tsukita, and S. Tsukita. 1993. The 220-kD protein colocalizing with cadherins in non-epithelial cells is identical to ZO-1, a tight junction-associated protein in epithelial cells: cDNA cloning and immunoelectron microscopy. *J. Cell Biol.* 121:491–502.

Joshi, H. C., M. J. Palacios, L. McNamara, and D. W. Cleveland. 1992. Gamma-tubulin is a centrosomal protein required for cell cycle-dependent microtubule nucleation. *Nature (Lond.).* 356:80–83.

Katsuya, H., Y. Ishimaru, M. Koono, and H. Hayashi. 1978. A light and electron microscopic study on complete dissociation of rat ascites hepatoma cells under activation of neutral protease and calcium depletion. *Virchows Arch. B Cell Path.* 27:159–172.

Kitamura, T., P. Jansen, C. Hardenbrook, Y. Kamimoto, Z. Gatmaitan, and I. M. Arias. 1990. Defective ATP-dependent bile canalicular transport of organic anions in mutant (TR−) rats with conjugated hyperbilirubinemia. *Proc. Natl. Acad. Sci. USA.* 87:3557–3561.

Koval, M., and R. E. Pagano. 1990. Sorting of an internalized plasma membrane lipid between recycling and degradative pathways in normal and Niemann-Pick, Type A fibroblasts. *J. Cell Biol.* 111:429–442.

Koval, M., and R. E. Pagano. 1991. Intracellular transport and metabolism of sphingomyelin. *Biochem. Biophys. Acta.* 1082:113–125.

Lake, J. R., V. Licko, R. W. Van Dyke, and B. F. Scharschmidt. 1985. Biliary secretion of fluid-phase markers by the isolated perfused rat liver. Role of transcellular vesicular transport. *J. Clin. Invest.* 76:676–684.

Le Bivic, A., M. Hirn, and H. Reggio. 1988. HT-29 cells are an *in vitro* model for the generation of cell polarity in epithelia during embryonic differentiation. *Proc. Natl. Acad. Sci. USA.* 85:136–140.

Lipsky, N. G., and R. E. Pagano. 1983. Sphingolipid metabolism in cultured fibroblasts: microscopic and biochemical studies employing a fluorescent ceramide analogue. *Proc. Natl. Acad. Sci. USA.* 80:2608–2612.

Lipsky, N. G., and R. E. Pagano. 1985. Intracellular translocation of fluorescent sphingolipids in cultured fibroblasts: endogenously synthesized sphingomyelin and glucocerebroside analogues pass through the Golgi apparatus en route to the plasma membrane. *J. Cell Biol.* 100:27–34.

Lowe, P. J., K. Miyai, J. H. Steinbach, and W. G. M. Hardison. 1988. Hormonal regulation of hepatocyte tight junctional permeability. *Am. J. Physiol.* 255:G454–G461.

Luzio, J. P., E. M. Bailyes, M. Baron, K. Siddle, B. M. Mullock, H. J. Geuze, and K. K. Stanley. 1986. The properties, structure, function, intracellular localisation and movement of hepatic 5′-nucleotidase. *In* Cellular Biology of Ectoenzymes. G. W. Kreutzberg, editor. Springer-Verlag, Berlin/Heidelberg. 89–116.

Mandel, L. J., R. Bacallao, and G. Zampighi. 1993. Uncoupling of the molecular 'fence' and paracellular 'gate' functions in epithelial tight junctions. *Nature (Lond.).* 361:552–555.

Matter, K., K. Bucher, and H.-P. Hauri. 1990. Microtubule perturbation retards both the direct and the indirect apical pathway but does not affect sorting of plasma membrane proteins in intestinal epithelial cells (Caco-2). *EMBO (Eur. Mol. Biol. Organ.) J.* 9:3163–3170.

Maurice, M., E. Rogier, D. Cassio, and G. Feldmann. 1988. Formation of

plasma membrane domains in rat hepatocytes and hepatoma cell lines in culture. *J. Cell Sci.* 90:79–92.

McRoberts, J. A., M. Taub, and M. H. Saier Jr. 1981. The Madin-Darby canine kidney (MDCK) cell line. *In* Functionally Differentiated Cell Lines. G. Sato, editor. Alan R. Liss, Inc., New York. 117–139.

Mevel-Ninio, M., and M. C. Weiss. 1981. Immunofluorescence analysis of the time-course of extinction, reexpression and activation of albumin production in rat hepatoma-mouse fibroblast heterokaryons and hybrids. *J. Cell Biol.* 90:339–350.

Motta, P., M. Muto, and T. Fujita. 1978. The liver. An atlas of scanning electron microscopy. Igaku-Shoin, Tokyo. 14 pp.

Nathanson, M. H., and J. L. Boyer. 1991. Mechanisms and regulation of bile secretion. *Hepatology.* 14:551–566.

Nathanson, M. H., A. Gautam, O. C. Ng, R. Bruck, and J. L. Boyer. 1992. Hormonal regulation of paracellular permeability in isolated rat hepatocyte couplets. *Am. J. Physiol.* 262:G1079–G1086.

Oda, M., V. M. Price, M. M. Fisher, and M. J. Phillips. 1974. Ultrastructure of bile canaliculi, with special reference to the surface coat and the pericanalicular web. *Lab. Invest.* 31:314–323.

Pagano, R. E. 1990. The Golgi apparatus: insights from lipid biochemistry. *Biochem. Soc. Trans.* 18:361–366.

Pagano, R. E., and O. C. Martin. 1988. A series of fluorescent N-acylsphingosines: synthesis, physical properties, and studies in cultured cells. *Biochemistry.* 27:4439–4445.

Phillips, M. J., C. Oshio, M. Miyairi, and C. R. Smith. 1983. Intrahepatic cholestasis as a canalicular motility disorder. Evidence using cytochalasin. *Lab. Invest.* 48:205–211.

Pinto, M., S. Robine-Leon, M.-D. Appay, M. Kedinger, N. Triadou, E. Dussaulx, B. Lacroix, P. Simon-Assmann, K. Haffen, J. Fogh, and A. Zweibaum. 1983. Enterocyte-like differentiation and polarization of the human colon carcinoma cell line Caco-2 in culture. *Biol. Cell.* 47:323–330.

Pisam, M., and P. Ripoche. 1976. Redistribution of surface macromolecules in dissociated epithelial cells. *J. Cell Biol.* 71:907–920.

Porvaznik, M., R. G. Johnson, and J. D. Sheridan. 1976. Intercellular junctions and other cell surface differentiations of H4-11E hepatoma cells in vitro. *J. Ultrastruct. Res.* 55:343–359.

Rindler, M. J., I. E. Ivanov, and D. D. Sabatini. 1987. Microtubule-acting drugs lead to the nonpolarized delivery of the influenza hemagglutinin to the cell surface of polarized Madin-Darby Canine kidney cells. *J. Cell Biol.* 104: 231–241.

Rodriguez-Boulan, E., P. J. Salas, M. Sargiacomo, M. Lisanti, A. Le Bivic, Y. Sambuy, D. Vega-Salas, and L. Graeve. 1989. Methods to estimate the polarized distribution of surface antigens in cultured epithelial cells. *Methods Cell Biol.* 32:37–56.

Rogier, E., D. Cassio, M. C. Weiss, and G. Feldmann. 1986. An ultrastructural study of rat hepatoma cells in culture, their variants and revertants. *Differentiation.* 30:229–236.

Rosenwald, A. G., and R. E. Pagano. 1993. Intracellular transport of ceramide and its metabolites at the Golgi complex: insights from short-chain analogs. *Adv. Lipid Res.* 26:101–118.

Rotman, B., and B. W. Papermaster. 1966. Membrane properties of living mammalian cells as studied by enzymatic hydrolysis of fluorogenic esters. *Proc. Natl. Acad. Sci. USA.* 55:134–141.

Sargiacomo, M., M. Lisanti, L. Graeve, A. Le Bivic, and E. Rodriguez-Boulan. 1989. Integral and peripheral protein composition of the apical and basolateral membrane domains in MDCK cells. *J. Membr. Biol.* 107:277–286.

Schell, M. J., M. Maurice, B. Stieger, and A. L. Hubbard. 1992. 5′ nucleotidase is sorted to the apical domain of hepatocytes via an indirect route. *J. Cell Biol.* 119:1173–1182.

Schneeberger, E. E., and R. D. Lynch. 1992. Structure, function, and regulation of cellular tight junctions. *Am. J. Physiol.* 262:L647–L661.

Scott, L. J., and A. L. Hubbard. 1992. Dynamics of four rat liver plasma membrane proteins and polymeric IgA receptor. Rates of synthesis and selective loss into the bile. *J. Biol. Chem.* 267:6099–6106.

Sellinger, M., and J. L. Boyer. 1990. Physiology of bile secretion and cholestasis. *Prog. Liver Dis.* 9:237–259.

Siddle, K., E. M. Bailyes, and J. P. Luzio. 1981. A monoclonal antibody inhibiting rat liver 5′-nucleotidase. *FEBS (Fed. Eur. Biochem. Soc.) Lett.* 128:103–107.

Spiegel, S., R. Blumenthal, P. H. Fishman, and J. S. Handler. 1985. Gangliosides do not move from apical to basolateral plasma membrane in cultured epithelial cells. *Biochim. Biophys. Acta.* 821:310–318.

Stearns, T., L. Evans, and M. Kirschner. 1991. Gamma-tubulin is a highly conserved component of the centrosome. *Cell.* 65:825–836.

Stevenson, B. R., and D. A. Goodenough. 1984. Zonulae occludentes in junctional complex-enriched fractions from mouse liver: preliminary morphological and biochemical characterization. *J. Cell Biol.* 98:1209–1221.

Stevenson, B. R., J. D. Siliciano, M. S. Mooseker, and D. A. Goodenough. 1986. Identification of ZO-1: a high molecular weight polypeptide associated with the tight junction (zonula occludens) in a variety of epithelia. *J. Cell Biol.* 103:755–766.

Tsukada, N., and M. J. Phillips. 1993. Bile canalicular contraction is coincident with reorganization of pericanalicular filaments and co-localization of actin and myosin-II. *J. Histochem. Cytochem.* 41:353–363.

van Meer, G., and K. Simons. 1986. The function of tight junctions in maintaining differences in lipid composition between the apical and the basolateral cell surface domains of MDCK cells. *EMBO (Eur. Mol. Biol. Organ.) J.* 5:1455–1464.

van Meer, G., E. H. K. Stelzer, R. W. Wijnaendts-van-Resandt, and K. Simons. 1987. Sorting of sphingolipids in epithelial (Madin-Darby canine kidney) cells. *J. Cell Biol.* 105:1623–1635.

van't Hof, W., and G. van Meer. 1990. Generation of lipid polarity in intestinal epithelial (Caco-2) cells: sphingolipid synthesis in the Golgi complex and sorting before vesicular traffic to the plasma membrane. *J. Cell Biol.* 111:977–986.

Vega-Salas, D. E., P. J. I. Salas, and E. Rodriguez-Boulan. 1987. Modulation of the expression of an apical plasma membrane protein of Madin-Darby canine kidney cells: cell–cell interactions control the appearance of a novel intracellular storage compartment. *J. Cell Biol.* 104:1249–1259.

Watanabe, N., N. Tsukada, C. R. Smith, and M. J. Phillips. 1991. Motility of bile canaliculi in the living animal: implications for bile flow. *J. Cell Biol.* 113:1069–1080.